BOOK OF FULL TEXT PROCEEDINGS TURKISH PHYSICAL SOCIETY
40th INTERNATIONAL PHYSICS CONGRESS (TPS40)
TPS40 (2024), Vol.06, No.03, pp.74-80.
ISBN:978-625-95049-3-3

A View of Coherent Elastic Neutrino-Nucleus Scattering

Mehmet Demirci[1, a)] and Onur Başlı[2, b)]

[1]*Department of Physics, Karadeniz Technical University, Trabzon TR61080, Türkiye*
[2]*Department of Physics, Bursa Uludağ University, Bursa TR16059, Türkiye*

[a)] *mehmetdemirci@ktu.edu.tr*
[b)] *onurbasli@uludag.edu.tr*

Abstract. Coherent elastic neutrino-nucleus scattering (CEνNS) is a neutral current process where neutrinos are scattered from a nucleus that acts as a single particle. It is difficult to observe experimentally the CEνNS process since the nuclear recoil energy reaches to low keV region. The process was firstly observed by the COHERENT experiment in 2017 with a CsI[Na] scintillating crystal detector using neutrinos from pion-decays-at-rest (πDAR). It was then also measured using a single-phase LAr and with a larger CsI[Na] detector. The detection of CEνNS has triggered both theoretical and experimental activities in high-energy physics, leading new constraints on physics scenarios beyond the SM. It has been widely used in searching for the weak mixing angle, non-standard neutrino interactions, the effective generalized interactions, light mediator models, the neutrino electromagnetic properties and dark-matter.

INTRODUCTION

Coherent elastic neutrino nucleus scattering (CEνNS) is a weak neutral current interaction process that was theoretically predicted half a century ago [1, 2, 3]. It is well defined at low energies within the Standard Model (SM) framework. The process is based on the principle that neutrinos are scattered out of the nucleus as a whole via the SM neutral gauge boson Z^0 at low momentum transfer, giving it a small recoil energy. In the CEνNS process, the neutrino interacts coherently with the nucleus without changing its internal state. The only experimental signature of this process is the recoil energy of the nucleus. The maximum nuclear recoil energy is limited by the kinematics of the elastic scattering:

$$T_{nr}^{max} = \frac{2E_\nu^2}{2E_\nu + m_N A} \approx \frac{2E_\nu^2}{m_N A} \tag{1}$$

where E_ν is the initial neutrino energy, m_N is the target nuclei mass and A is the atomic number of nucleus. Neutrinos interact coherently with the nucleus, with nuclear recoil energies at low momentum transfer in the range of a few keV. This makes it experimentally challenging to detect. For this reason, Freedman pointed out that experimental detection of CEνNS would be an "act of hubris" because of the associated with "grave experimental difficulties" [1]. On the other hand, Eq. (1) indicates that lighter target nuclei increase the value of T_{nr}^{max} produced in the detector.

The keV scale low-threshold required to observe the CEνNS signal has used from recent advances in detector technologies primarily driven by searches for dark matter that lie in the same target recoil range. The recoil energy is usually collected in the form of ionized charge or scintillation photons, which depend on the detector technology. The first experimental observation of the CEνNS process was made by the COHERENT Collaboration in 2017 [4]. In their first measurement, they used neutrinos emerging from pion decay at rest (πDAR) by the Spallation Neutron Source (SNS) at Oak Ridge National Laboratory with a CsI[Na] scintillating crystal detector [4, 5] and then carried out a second one using a LAr detector [6]. The experiment has updated the CsI data analysis with higher statistics and a better understanding of the experimental systematics [7]. This success has motivated both theoretical and experimental scientific activities related to CEνNS.

The interesting aspect of CEνNS is that it has important implications in nuclear physics, particle physics and astrophysics. It provides useful information about the nuclear structure, especially the neutron density distribution in

ISBN:978-625-95049-3-3

the nucleus, which surprisingly is still unknown for most nuclei. It also gives information about the exact value of the neutrino neutral-current interaction at low energy, measured by a concept called the "weak mixing angle" [8]. Moreover, CEνNS is sensitive to effects of physics beyond the SM (BSM) such as the neutrino electromagnetic properties [9, 10], neutrino interactions mediated by new neutral bosons [11, 12], and, in general, the neutrino neutral current non-standard interactions (NSI) [13, 14]. On the other hand, the observation of astrophysical neutrino fluxes will provide new insight into the supernovas [15], the primordial black holes [16] and the collapsing supermassive stars [17].

The remainder of this study is organized as follows. First of all, we list low-energy neutrino sources for CEνNS. Then, we briefly present the general formalism of calculating the CEνNS cross section. Next, we discuss how the CEνNS experiments could be used as a testing ground for SM weak neutral current interactions. Finally, we summarize our study in the light of new developments in the field.

LOW ENERGY NEUTRINO SOURCES

The CEνNS process is dominant only at neutrino energies of tens of MeV. These neutrinos come from a variety of sources, including the accelerator-induced decay at rest sources, nuclear reactors, and astrophysical sources such as supernovae and solar neutrinos. Neutrinos from the stopped pion sources span energies on the scale of tens of MeV and are nearly ideal for studying CEνNS. So far, CEνNS only has been observed with neutrinos from the decay at rest sources and not in others. Therefore, it focuses primarily on neutrinos originating from a pion decay at rest source.

Stopped pion source

Spallation sources produce $\pi^{\pm}$ via proton-nuclei collisions. Most of the produced π^{-} are captured by nuclei, and hence do not decay to produce neutrinos. On the other hand, the π^{+} lose energy and decay at rest, to produce monoenergetic ν_{μ} neutrinos with energy 29.8 MeV. The dominant neutrino production comes from the following prompt decay

$$\pi^{+} \rightarrow \mu^{+} + \nu_{\mu} \quad (\text{decay time: } \tau \sim 26\, ns) \tag{2}$$

followed by a three-body delayed decay of muons

$$\mu^{+} \rightarrow e^{+} + \nu_{e} + \overline{\nu_{\mu}} \quad (\text{decay time: } \tau \sim 2.2\, \mu s) \tag{3}$$

These produce a well-known spectrum shape. The spectral functions are defined by

$$\phi_{\nu_{\mu}}(E_{\nu}) = \frac{2m_{\pi}}{m_{\pi}^2 - m_{\mu}^2}\,\delta\left(1 - \frac{2E_{\nu}\, m_{\pi}}{m_{\pi}^2 - m_{\mu}^2}\right) \tag{4}$$

$$\phi_{\nu_{e}}(E_{\nu}) = \frac{192}{m_{\mu}}\left(\frac{E_{\nu}}{m_{\mu}}\right)^2\left(\frac{1}{2} - \frac{E_{\nu}}{m_{\mu}}\right) \tag{5}$$

$$\phi_{\overline{\nu}_{\mu}}(E_{\nu}) = \frac{64}{m_{\mu}}\left(\frac{E_{\nu}}{m_{\mu}}\right)^2\left(\frac{3}{4} - \frac{E_{\nu}}{m_{\mu}}\right) \tag{6}$$

For a pion decay at rest source, the maximum neutrino energy is $E_{\nu}^{max} = m_{\mu}/2$ where $m_{\mu} = 105{,}65$ MeV is the muon mass. Pion decay at the rest frame (πDAR) is prominent at low energies, and the high-energy peaks are due to pion decay in motion. In Fig.1, we show flux of πDAR neutrinos. Here, ν_{μ} has a 29.8 MeV monoenergetic, whereas the energies of ν_{e} and $\overline{\nu_{\mu}}$ ranges up to $m_{\mu}/2$.

ISBN:978-625-95049-3-3

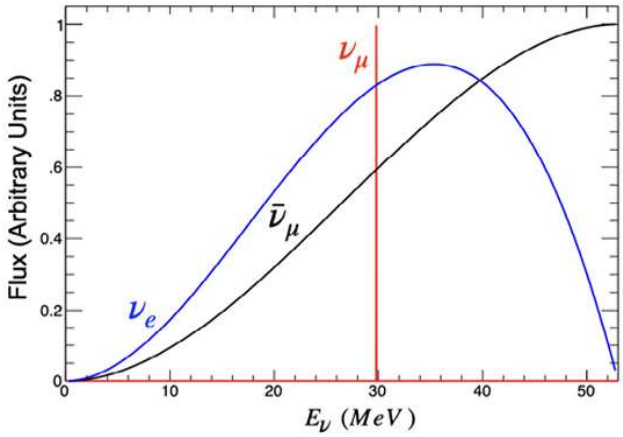

FIGURE 1. Neutrino energy spectra of pion decay at rest neutrinos [18].

Nuclear reactors

Nuclear reactors have long been used as sources of the anti-electron neutrinos $\bar{\nu}_e$. Reactor neutrinos are detected by observing both the outgoing positron and the neutron produced together using the inverse beta decay of $\bar{\nu}_e p \rightarrow e^+ n$. The characteristic neutrino energy is $\lesssim$ 1 MeV, which is nearly an order of magnitude less than the neutrinos produced by accelerator sources. Due to these low energies the coherent condition of CEνNS for nuclear recoil is largely maintained throughout the entire reactor energy region, so that there is no dependence on the internal structure of the nucleus [19].

Solar neutrinos

One of the most intense sources of neutrinos on the Earth are solar neutrinos, which have been comprehensively used since their first observations [20]. These neutrinos are produced inside the Sun via nuclear fusion processes. These are usually grouped as the proton-proton (pp) chain or the carbon-nitrogen-oxygen (CNO) cycle. In the pp chain, neutrinos are produced from several nuclear reactions called as the hep, pp, pep, ^{7}Be and ^{8}B. In the CNO cycle, neutrinos mainly come from decays of ^{13}N, ^{15}O, and ^{17}F. The solar neutrino flux spectrum $d\Phi(E_\nu)/dE_\nu$ from the high metallicity solar neutrino model BS05(OP) [21] is shown in Fig.(2).

Solar neutrino measurements are tightly connected with the discovery of flavor conversion and the matter effect on the neutrino dispersion which is achieved through the observation of different processes such as neutral current, charged current and elastic scattering.

Supernova neutrinos

Star-collapse neutrinos were first (and so far, only) observed in 1987. Neutrinos of ν_e, $\bar{\nu}_e$, and ν_μ/ν_τ flavors are thought to have emerged from the core of the supernova at temperatures with energies of about 3, 5, and 8 MeV, respectively [22]. Although neutrino detectors have been in operation for the past three decades since SN 1987A, no detection of neutrinos from a Galactic supernova has yet been made [23]. Detectors sensitive to CEνNS could play an important role in extracting information from supernova neutrinos. Through the CEνNS channel, and neutrinos flavors will be accessible [24]. It has been recognized for many years that this provides important information about the nature of stellar collapse [25].

ISBN:978-625-95049-3-3

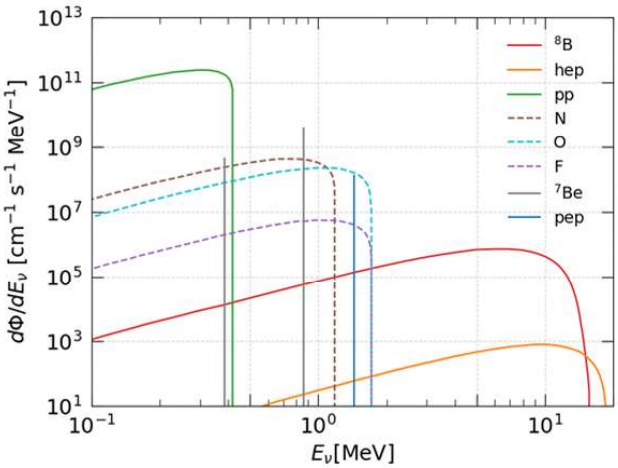

FIGURE 2. Solar neutrino energy spectra for the BS05(OP) model. Neutrino fluxes from the pp chain are shown as continuous lines, while the CNO neutrino fluxes are shown as dashed lines [12].

CEνNS IN THE FRAMEWORK OF THE SM

The CEνNS process is well predicted in the framework of the SM. This occurs when a neutrino scatters off the entire nucleus, exchanging a Z^0 boson, transferring low momentum to the nucleus as a whole with small recoil energy, but without creating any internal excitation in the nucleus. It is elastic in the sense that no new particles are created in the scattering and the residual nucleus stays in its ground state [26]. For neutrinos carrying energies of a few tens of MeV and scattered from moderately sized nuclei, a dominant fraction of the interactions is expected to be of the coherent type.

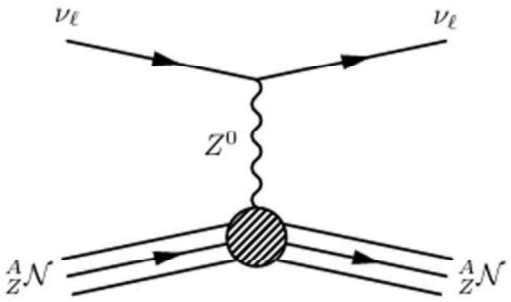

FIGURE 3. Feynman diagram for CEνNS in the SM.

At the tree-level in the SM, the Feynman diagram for the CEνNS process is shown in Fig.3, where the subscript ℓ denotes to the neutrino flavour $\ell = e, \mu$ or τ. The matrix element of the process $\nu(p_1)N(p_2) \rightarrow \nu(p_3)N(p_4)$ is written as

$$M = \frac{G_F}{2\sqrt{2}} Q_{\text{SM}}\, \bar{\nu}(p_3)\gamma^\mu(1-\gamma^5)\nu(p_1)\, \bar{u}(p_4)\gamma_\mu u(p_2) \tag{7}$$

where p_1, p_2, p_3 and p_4 represent the four-momenta vectors of the incoming and outgoing neutrinos and the nucleus, respectively. Here, the nucleus is considered as a Dirac particle. The weak nuclear charge Q_{SM} is given as

$$Q_{SM} = g_V^p\, ZF_Z(|\vec{q}|^2) + g_V^n\, NF_N(|\vec{q}|^2) \tag{8}$$

ISBN:978-625-95049-3-3

where the transfer momentum $\vec{q}$ is proportional to $|\vec{q}| \lesssim \frac{1}{R}$ with the typical nuclear size R. The proton and neutron vector couplings are defined by

$$g_V^p = \frac{1}{2}(1 - 4sin^2\theta_W) \quad \text{and} \quad g_V^n = -\frac{1}{2} \tag{9}$$

respectively. For the weak-mixing angle θ_W, we use the value of $sin^2\theta_W = 0.23863$ [27] (at low momentum transfer in the $\overline{MS}$ scheme). Although the proton contribution is small ($\simeq 0.0229$), this contribution depends on the weak mixing angle. On the other hand, the SM cross section of the process is flavor independent at tree level. There are flavor dependencies in the small loop corrections, however they have no significant impact for the current sensitivities [28]. The weak nuclear form factors are given by $F_Z(|\vec{q}|^2)$ and $F_N(|\vec{q}|^2)$, which describe the nucleon complex structure of the target nucleus. The same form factor is generally taken for both proton and neutron, namely $F_Z \simeq F_N = F$. The Helm parametrization [29] for the form factor is defined by

$$F(|\vec{q}|^2) = 3\frac{j_1(|\vec{q}|R_0)}{|\vec{q}|R_0} e^{-\frac{1}{2}|\vec{q}|^2 s^2} \tag{10}$$

where $j_1(x) = sinx/x^2 - cosx/x$ is the first-order spherical Bessel function and the three-momentum transfer is $|\vec{q}| = \frac{\sqrt{2m_N T_{nr}}}{197.3}$ fm^{-1}. The diffraction radius is defined by $R_0^2 = \frac{5}{3}R^2 - 5s^2$, with the nuclear radius $R = 1.23\,A^{1/3}$ and the surface thickness $s = 0.9$ fm. The CEνNS process is focused in the region $Q \leq 50$ MeV ($Q^2 \equiv -q^2 = 2m_N T_{nr}$) (Fig.4). For this scale, it can be taken to be $|F(|\vec{q}|^2)|^2 \approx 1$, which is called "full coherence".

The measurable CEνNS differential cross section of a neutrino with a spin-zero nucleus in the SM is given by

$$\left[\frac{d\sigma_{\nu_\alpha - N}}{dT_{nr}}\right]_{SM} = \frac{G_F^2 m_N}{4\pi}\left(1 - \frac{m_N T_{nr}}{2E_\nu^2}\right)[N - (1 - 4sin^2\theta_W)Z]^2 |F(|\vec{q}|^2)|^2 \tag{11}$$

Note that if there are several stable isotopes for the target material, the cross section should be weighted averaged according to the natural abundance. Figure 4 shows the effect of form factor for the several targets, which are particularly the preferred nuclei in detector (TEXONO, CONUS) and accelerator (COHERENT) neutrino experiments. Heavier target, CsI, penetrate deeper than the lighter one, Si.

The cross section of CEνNS process is larger than ones of the other neutrino interactions at the same neutrino energy. Also, if the $sin^2\theta_W$ value is substituted in Eq.(11), the cross section will be proportional to N^2. A deviation from $\sigma_{SM} \propto N^2$ prediction can be a signature of the BSM physics.

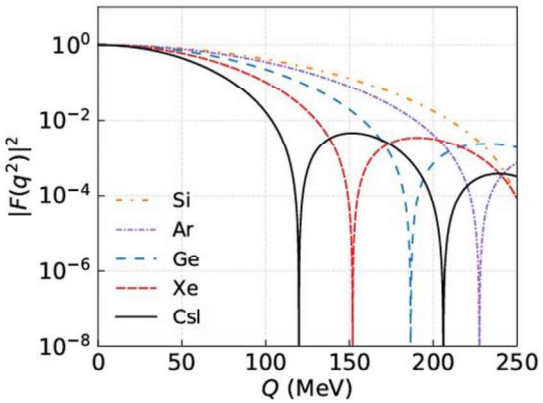

FIGURE 4. The nuclear form factor contribution for several target nuclei as a function of transfer momentum.

CONCLUSION

The recent experimental observation of CEνNS at a πDAR neutrino source has motivated many research fields. This new way of detecting neutrinos has broader implications for frontier communities spanning particle physics, nuclear physics, astrophysics, and beyond. By taking advantage of the fact that the CEνNS cross section is many times larger, new physics can be probed with relatively small detectors. CEνNS offer a natural window to probe light, weakly-coupled, new physics in the neutrino sector.

ACKNOWLEDGMENTS

This work was supported by the Scientific and Technological Research Council of Türkiye (TÜBİTAK) under Project 123F186.

REFERENCES

1. D. Z. Freedman, "Coherent effects of a weak neutral current," Phys. Rev. D 9, 1389–1392 (1974).
2. D. Tubbs and D. Schramm, "Neutrino opacities at high temperatures and densities," Astrophysical Journal 201, 467–488 (1975)
3. A. Drukier and L. Stodolsky, "Principles and applications of a neutral-current detector for neutrino physics and astronomy," Phys. Rev. D 30(11), 2295 (1984).
4. D. Akimov et. al. [Coherent Collaboration], "Observation of coherent elastic neutrino-nucleus scattering," Science 357, 1123–1126 (2017).
5. D. Akimov et. al. [Coherent Collaboration]," COHERENT Collaboration data release from the first observation of coherent elastic neutrino-nucleus scattering" arXiv:1804.09459 [nucl-ex].
6. D. Akimov et. al. [Coherent Collaboration], "First measurement of coherent elastic neutrino-nucleus scattering on argon," Phys. Rev. Lett. 126, 012002 (2021).
7. D. Akimov et. al. [Coherent Collaboration], "Measurement of the coherent elastic neutrino-nucleus scattering cross section on csi by coherent," Phys. Rev. Lett. 129, 081801 (2022).
8. M.Cadeddu and F. Dordei, "Reinterpreting the weak mixing angle from atomic parity violation in view of the Cs neutron rms radius measure ment from COHERENT," Phys. Rev. D 99(3), 033010 (2019).
9. C. Giunti, K. A. Kouzakov, Y.-F. Li, A. V. Lokhov, A. I. Studenikin, and S. Zhou, "Electromagnetic neutrinos in laboratory experiments and astrophysics," Ann. Phys. (Berlin) 528, 198 (2016).
10. A. I. Studenikin and K. A. Kouzakov, "The electromagnetic properties of the neutrino as a window to new physics," Moscow University Physics Bulletin 75(5), 379–397 (2020).
11. P. Coloma, M. C. Gonzalez-Garcia, M. Maltoni, J. P. Pinheiro, and S. Urrea, "Constraining new physics with borexino phase-ii spectral data," J. High Energy Phys. 07, 138 (2022).
12. M. Demirci and M. F. Mustamin, "Solar neutrino constraints on light mediators through coherent elastic neutrino-nucleus scattering," Phys. Rev. D 109, 015021 (2024).
13. J. Barrancon, A. Bolanos, E. A. Garces, O. G. Miranda, and T. Rashba, "Tensorial nsi and unparticle physics in neutrino scattering," Int. J. Mod. Phys. A 27, 1250147 (2012).
14. M. F. Mustamin and M. Demirci, "Study of non-standard neutrino interactions in future coherent elastic neutrino-nucleus scattering experiments," Braz. J. Phys. 51, 813 (2021).
15. X.-R. Huang, S. Zha, and L.-W. Chen, "Supernova preshock neutronization burst as a probe of non-standard neutrino interactions," Astrophys. J. Lett. 923, L26 (2021).
16. R. Calabrese, D. G. Fiorillo, G. Miele, S. Morisi, and A. Palazzo, "Primordial black hole dark matter evaporating on the neutrino floor," Phys. Lett. B 829, 137050 (2022).
17. V. Munoz, V. Takhistov, S. J. Witte, and G. M. Fuller, "Exploring the origin of supermassive black holes with coherent neutrino scattering," J. Cosmol. Astropart. Phys. 11, 020 (2021).
18. D. Baxter, "Coherent elastic neutrino-nucleus scattering at the european spallation source," J. High Energy Phys. 2, 1–38 (2020).
19. V.A.Bednyakov and D.V.Naumov, "Coherency and incoherency in neutrino-nucleus elastic and inelastic scattering," Phys. Rev. D 98, 053004 (2018).
20. J. R. Davis, D. S. Harmer, and K. C. Hoffman, "Search for neutrinos from the sun," Phys. Rev. Lett. 20, 1205 (1968).

21. J. N. Bahcall, A. M. Serenelli, and S. Basu, "New solar opacities, abundances, helioseismology, and neutrino fluxes," Astrophys. J. Lett. L85, 621 (2005).
22. G. G. Raffelt, M. T. Keil, R. Buras, H.-T. Janka, and M. Rampp, eds., in Neutrino oscillations and their origin., All ACM Conferences No. 2003 (4th International Workshop, NOON2003, Kanazawa, Japan, 2003).
23. M.Ikeda and Super-Kamiokande, "Search for supernova neutrino bursts at super-kamiokande," Astrophys. J. 669, 519 (2007).
24. L. Pattavina, N. F. Iachellini, and I. Tamborra, "Neutrino observatory based on archaeological lead," Phys. Rev. D 102, 063001 (2020).
25. D. Z. Freedman, D. N. Schramm, and D. L. Tubbs, "Weak neutral current and its effects in stellar collapse," Ann. Rev. Nucl. Part. Sci. 27, 167 (1977).
26. V. Pandey, "Recent progress in low energy neutrino scattering physics and its implications for the standard and beyond the standard model physics," Progress in Particle and Nuclear Physics 134, 104078 (2024).
27. R. L. Workman et. al., [Particle Data Group] PTEP 2022, 083C01 (2022).
28. O. Tomalak, P. Machado, V. Pandey, and R. Plestid, "Inelastic and elastic scattering of 187-mev electrons from selected even-even nuclei," J. High Energy Phys. 02, 097 (2021).
29. R. H. Helm, "Testing neutrino electromagnetic properties at current and future dark matter experiments," Phys. Rev. 104, 1466–1475 (1956).